

Analytical Model for Simulation of Forming Process & Residual Stresses in Helical Springs

— Part 2

by:

Dr.-Ing. Vladimir Kobelev
Muhr und Bender KG
P.O. 360
D-57427, Attendorn, Germany
www.mubea.com

Residual stress can have a great effect on the properties of a material. This article offers a mathematical theory of residual stresses and strains in helical springs that allows calculating stresses on all manufacturing process steps, particularly during coiling and presetting.

In Part 1 of this article, the author looked at the Isotropic Work-Hardening Stress-Strain Law and the theory of elastic-plastic combined bending and torsion of a naturally curved and twisted bar. Complete mathematical analyses were offered.

In Part 2 of this article, the author looks at the theory of elastic-plastic combined bending and torsion of naturally curved and twisted bar, application of combined bending and torsion theory for simulation of preset for helical springs and the conclusions.

Application of Combined Bending & Torsion Theory for Coiling Simulation

Residual Stresses & Modeling of Spring Manufacturing Process

The simplest definition of residual stresses is as follows: the stresses that remain within a part or a component after the part or component has been deformed and all external forces have been removed.

More specifically, the deformation must be nonuniform across the material cross-section in order to give rise to residual stresses. The deformation can result not only from forming operations, but also from thermal processes.

Phase transformations during heat treating are

known to induce sufficient strain to result in plastic deformation, thereby giving rise to residual stresses. In this article, we determine analytically the residual stress, which appears in the cylindrical rod after simultaneous plastic torsion and bending.

One of the principal foundations of mathematical theory of conventional plasticity for rate-independent metals is that there exists a well-defined yield surface in stress space for any material point under deformation.

A material point can undergo additional plastic deformation if the applied stresses are beyond current yield surface, which is generally referred as plastic loading. If the applied stress state falls within or on the yield surface, the metal will deform elastically only and is undergoing elastic unloading.

Although it has been always recognized throughout the history of development of plasticity theory that there is indeed inelastic deformation accompanying elastic unloading, which leads to a metal's hysteretic behavior. Its effects are usually negligible and are ignored in the mathematical treatment.

In the subsequent section of this article we investigate the two manufacturing processes (the coiling and the presetting), analytically.

Stresses During Plastic Coiling & Subsequent Elastic "Spring-Back" of Spring Wire

A cylindrical solid bar with circular cross-section of length L is loaded during the spring coiling from a stress-free state by terminal bending moment and the terminal twisting moment. For the

straight bar in its free state prior to coiling, one coil of the resulted helical spring is shown in **Figure 3**. The plastic stresses during the manufacturing and residual stresses in helical springs are calculated using the analytical formulas in *Part 1* of this article.

In the moment of coiling, the spring wire undergoes simultaneous bending and torsion. Consider a helical spring with the constant coiling radius and pitch. At the moment of coiling, when the ultimate plasticiza-

tion occurs, the coiling radius is assumed to be R_o .

The pitch of one coil at the moment of coiling is H_o . The local shape of the spring at the moment of coiling is a circular helix²¹. This is shown below in **Figure 5**.

The mathematical analysis of stresses during the plastic coiling and subsequent elastic “spring-back” of the spring wire is seen in **Figure 5** and in **Figure 6**.

Fig. 5 – Local shape of the spring at moment of coiling is a circular helix.

The local shape of the spring at the moment of coiling is a circular helix:

$$X = R_o \cos t, Y = R_o \sin t, Z = H_o t.$$

The immediate curvature κ_o and torsion w_o of the helix at the moment of coiling is

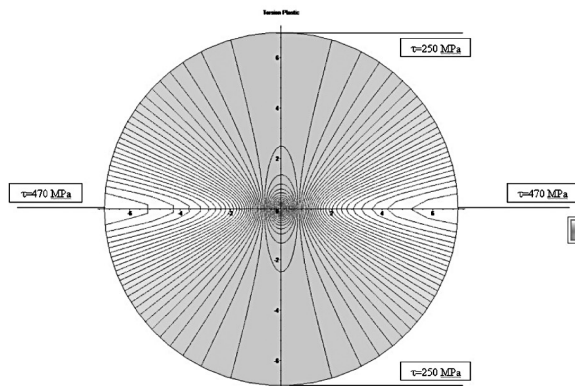
$$\kappa_o = \frac{R_o}{R_o^2 + H_o^2}, \quad w_o = \frac{H_o}{R_o^2 + H_o^2}.$$

The angle of twist per unit length in terms of torsion is $\theta_o = (2\pi)^{-1} w_o$.

In the moment, which follows immediately after coiling, the wire unloads elastically and forms the helical spring with unloaded curvature κ_A and torsion w_A . The unloaded curvature and torsion of the wire are

$$\kappa_A = \frac{R_A}{R_A^2 + H_A^2}, \quad w_A = 2\pi\theta_A = \frac{H_A}{R_A^2 + H_A^2}.$$

With these values, we calculate finally the unloaded radius R_A and pitch H_A of the spring “as coiled” respectively as



Shear stress in the cross section at maximal plasticization state in the moment of coiling

$$R_A = \frac{\kappa_A}{\kappa_A^2 + w_A^2}, \quad H_A = \frac{w_A}{\kappa_A^2 + w_A^2}.$$

Analytical Model for Simulation of Forming Process ...continued

Fig. 6 — Stresses during the plastic coiling and subsequent elastic “spring-back” of springwire.

For comparison, we use the experimental measurements of residual stresses in cold-coiled helical compression springs. The comparison is performed for as-coiled springs in central coils of reported diameter $2R_A = 160mm$ and pitch $H_A = 100mm$. For the spring manufacturing the Cr-Si wire is used. The diameter is $2r = 14mm$. The calculation results for plastic state in the spring material during manufacturing process are shown on the Figs. 4-8. The maximal plastic bending moment is 741 Nm. The plastic torque moment is 193 Nm.

The unloaded pitch is $H_O = 109mm$ and the radius is $2R_O = 144mm$. For simulation we use the functional modified stress-strain relations with $k = \frac{1}{2}$. The stress components and equivalent stress at the state of maximal plasticization are shown on the Fig. 3-6. The shear stress $\tau_{rz} = \sqrt{\tau_{xz}^2 + \tau_{yz}^2}$ over the cross-section is demonstrated on Fig. 3. The maximum of the shear stress is 170 MPa. In the centre of the cross section the stress vanishes. With the increasing radius the stress increases at first linearly with radius of the observation point, but on the outer surface of the rod the bending dominates, such that the shear stress stagnates. The normal axial stress σ_z at the maximal plasticization point $\alpha = 1$ increases from the value $\sigma = -1800MPa$ on the outmost outer point of the spring body ($x = -r$) to the value $\sigma = 1800MPa$ on the inner point ($x = r$). At $x = 0$ the bending stress disappears. The distribution of bending stress is mirror-symmetric due to the neutral axis $x = 0$.

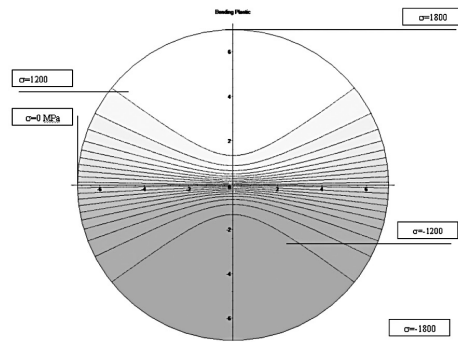


Fig. 4 - Axial normal stress in the cross section at maximal plasticization state in the moment of coiling

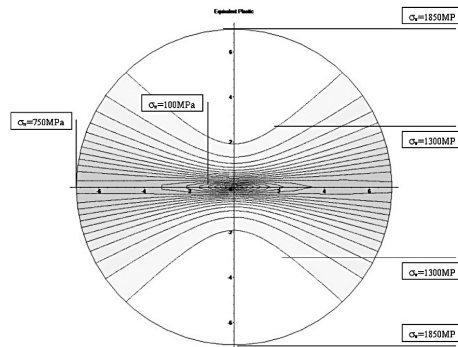


Fig. 5 - Equivalent stress in the cross section at maximal plasticization state in the moment of coiling

The equivalent stress (Fig. 4) in the spring cross-section is symmetric due to the neutral axis $x = 0$. The maximal value $\sigma_v = 1850MPa$ is attained on the outmost outer and inner points of the cross section. In the centre of the cross-section both shear and axial stress disappear, such that the equivalent stress vanishes. The plots of equivalent, shear and bending stresses on the outer contour of the circular cross-section are given on Fig. 6. The next figures (Fig.7-11) show components and equivalent stress at the final unloaded state of spring (spring as-coiled).The equivalent residual stress is plotted on the Fig. 7. The equivalent stress in the unloaded state over the spring cross-section is also symmetric due to the neutral axis $x = 0$, but its maximal value is located in the inner regions of the cross-section.

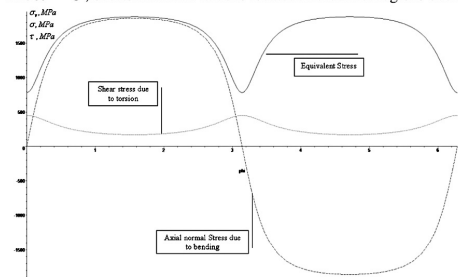


Fig. 6 - Plastic stresses on the contour of the cross-section at maximal plasticization state in the moment of coiling

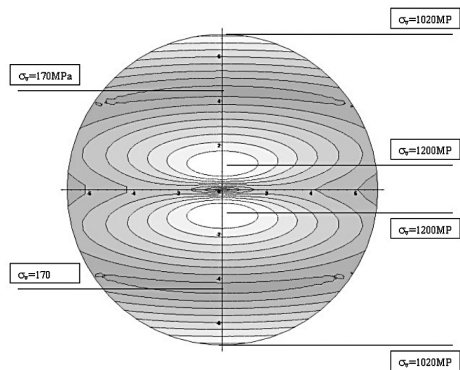


Fig. 7 - Residual equivalent stress at the unloaded state immediately after coiling (spring "as coiled")

The graph of residual shear stress and the axial stress are on the Fig. 8 and Fig. 9 correspondingly. The plots of equivalent, shear and bending stresses on the outer contour of the circular cross-section are given on Fig. 10.

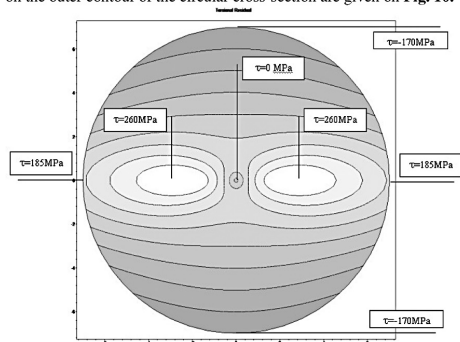


Fig. 8 - Residual shear stress at the unloaded state immediately after coiling (spring "as coiled")

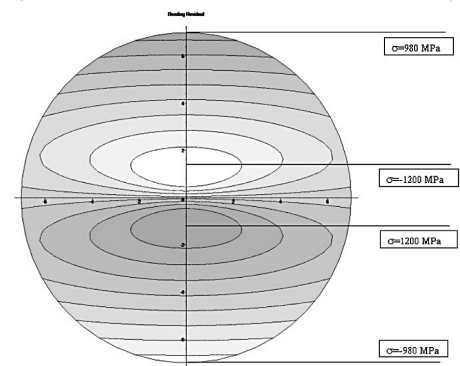


Fig. 9 - Residual axial normal stress at the unloaded state immediately after coiling (spring "as coiled")

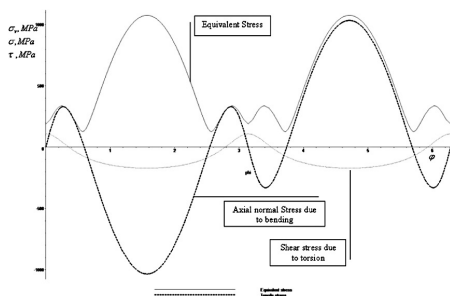


Fig. 10 - Residual stresses on the contour of the cross-section at the unloaded state immediately after coiling (spring "as coiled")

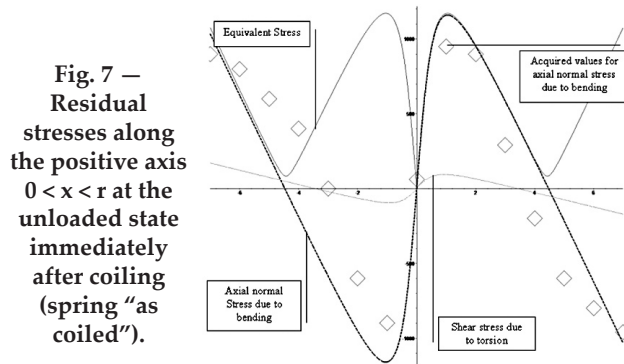
The profile of equivalent, shear and bending stresses along the $y = 0$, also $-r < x < r$ is plotted on the Fig. 7 on next page.

The figures demonstrate that the maximal equivalent, shear and bending stresses are located in the inner region of the cross section and are approximately 10-15% higher, than the corresponding maximal stress in the outer regions and on the surface of the cross-section. The simulated values of axial stress demonstrate an excellent correlation to the acquired values for axial normal stress due to bending, reported in the cited paper of MATEJICEK et al.

Application of Combined Bending & Torsion Theory for Simulation of Preset for Helical Springs

Unstressed Helical Compression Springs

The primary loading of helical compression springs is in torsion. This means that the wire will see tensile stresses oriented 45° to the wire axis and compressive stresses oriented 90° to the tensile stresses. The tensile applied stress has components in both the longitudinal and transverse directions. Therefore, a helical compression spring will be adversely impacted by both longitudinal and hoop residual stresses from wire drawing, hoop stresses from oil quenching and tensile bending stresses on the inside diameter from coiling.



The resulting residual stresses can be considerably reduced by the presetting and stress-relieving following the cold coiling. Presetting of helical compression springs consists of compressing the spring to a point at which plastic deformation occurs. Provided stress levels are sufficiently high to induce plastic deformation, this is typically carried out by compressing springs to or very near solid height. As a minimum, the springs should be compressed below the minimum operating height. This compression places the wire in torsion sufficient to induce plastic deformation in the outer fibers. The residual stress state is not uniform around the wire cross-section because the curvature of the wire alters the stress state from pure torsion during the compression.

The modeling of presetting process accounts the cyclic plastic loading. Classical plasticity theory is based on the concept of the yield surface. The movement of the yield surface under cyclic loading is described by the kinematical hardening rule and the dimensional change of the yield surface is described by the isotropic hardening rule.

The residual strains at the state of complete elastic unloading after active presetting could be obtained immediately subtracting the elastic stresses from stress components at the state of maximal presetting compression. Since the residual stress is mainly in torsion,

there will be a tensile component and a compressive component each at 45° to the wire axis. As was the case with the simple beam in bending example, the orientation of the residual stress is opposite to the orientation of the applied stress. Therefore, if loads in service are applied in the direction of the presetting load, the residual stresses from presetting will provide a net reduction in total stress under the service load.

For simulation of preset process, consider the unstressed helical compression spring with a central line of a curve with constant curvature and tortuosity. We use the index A to mark the geometry in the unstressed state, assuming that the residual stresses disappear during annealing process. Thus, the central line represents the helix traced on a right circular cylinder.

The angle which the tangent at any point of the unstressed helix makes with a plane at right angles to this axis is α_A (pitch angle). Let the R_A be the radius of cylinder on which helix lies. Then the curvature K_A and the measure of tortuosity θ_A (the angle of twist per unit length) of unstressed spring are given by the equation:

$$\kappa_A = \frac{\cos^2 \alpha_A}{R_A}, \theta_A = \frac{\sin \alpha_A \cos \alpha_A}{R_A}.$$

The mathematical analysis for the state of maximum plasticization during preset is given in Figure 8.

The mathematical analyses for elastic spring-back of helical spring and residual stresses after preset, and the residual stresses in helical springs after preset are given in Figure 9.

Conclusions

In this article, we simulate analytically two essential steps of spring manufacturing, namely the coiling and preset of the helical spring:

- The coiling process is the deformation of the initially straight rod to the helix. During this forming process the material flows plastically. Immediately after the moment of coiling the spring-back occurs. The residual stresses appear namely in the moment of elastic spring-back, which follows the plastic coiling of the spring. The formed coils are then stress relieved in a furnace, such that the relaxation process occurs and residual stresses disappear.
- Presetting a spring by bulldozing causes yielding. During this forming process the material flows plastically once again. On release, the spring-back of wire takes place and the surface is left with a residual shear stresses site in sign to the in-service load stress, thus clearly improving fatigue properties.

A list of symbols used in this article is presented in Table 1. For more information, contact the author or visit the website: www.mubea.com

Table 1. List of Symbols Used in this Article.

R_o	Radius at the moment of coiling (coiling radius)
H_o	Pitch of one coil at the moment of coiling
κ_o	Curvature of the helix at the moment of coiling
w_o	Torsion of the helix at the moment of coiling
$\theta_o = (2\pi)$	The angle of twist per unit length (measure of tortuosity) at the moment of coiling
α_A	Pitch angle of unstressed spring
R_A	The radius of unstressed spring
κ_A	Curvature of unstressed spring
θ_A	Measure of tortuosity of unstressed spring
σ_{zz}^B	Normal stress in the state B of maximal plasticization
τ_{rz}^B	Shear stress in the state B of maximal plasticization
α_B	Pitch angle of spring in the state at full stroke during preset
R_B	Radius of spring in the state at full stroke during preset
κ_B	Curvature of spring in the state at full stroke during preset
θ_B	Measure of tortuosity of spring in the state at full stroke during preset
F_p	Axial force of helical spring at preset
K_B	Couple of helical spring at preset
σ_{zz}^C	Normal residual stress in unloaded state C
τ_{rz}^C	Shear residual stress in unloaded state C
α_C	Pitch angle of helix in the unloaded state after preset
R_C	Radius of helix in the unloaded state after preset
κ_C	Curvature of helix in the unloaded state after preset
θ_C	Measure of tortuosity of helix of the unloaded state after preset
M_p	Bending moment in spring wire during the active plastic loading
T_p	Torsion moment in spring wire during the active plastic loading
M_e	Bending moment in spring wire during the elastic unloading
T_e	Torsion moment in spring wire during the elastic unloading
m_B	Bending moment in spring wire at the state of maximal plasticization
t_B	Torsion moment in spring wire at the state of maximal plasticization
$J_p = \pi r^4 / 4$	Polar moment of the circle with radius r
$J = \pi r^4 / 4$	Bending moment of the circle with radius r
G, E, ν	Elastic constants of isotropic elastic material
K	Plastic yield strain
ϵ_p	Plastic yield stress
$\sigma_p = E\epsilon_p$	Plastic yield stress
k	Hardening exponent
G_m	Secant modulus
$p^{(k)}, Q^{(k)}$	Dimensionless functions in plastic moment-strain relations
λ, μ	Dimensionless parameters
$q_{ii}^{(k)}, p_{ii}^{(k)}$	Dimensionless functions
...	

References:

¹ *Residual stresses in science and technology*, Eds. Macherauch E., Hauk V. DGM, Germany, 1986
² *Residual stresses*, Eds Noyan I.C., Cohen J.B. Springer-Verlag, Stuttgart, 1987

³ *Manual on Design and Application of Helical and Spiral Springs SAE HS-795*, SAE International, Warrendale, PA, 1997
⁴ Wahl A.M.: *Mechanical Springs*, McGraw-Hill, New York, 1963
⁵ Matejcek J., Brand P.C., Drews A.R., Krause A., Lowe-Ma C.: *Residual stresses in cold-coiled helical compression springs for automotive suspensions measured by neutron diffraction. Materials Science and Engineering A* 367, 306–311, 2004
⁶ Hencky, H.: *Zur Theorie plastischer Deformationen und der hierdurch im Material hervorgerufenen Nachspannungen*, Z. Angew. Math. Mech., Vol. 4, pp. 323-334, 1924.
⁷ Ilyushin, A. A.: *Theory of plasticity at simple loading of the bodies exhibiting plastic hardening*, Prikl. Mat. Mekh., Vol. 11, 291, 1947.
⁸ Ilyushin, A. A.: *Plasticity. Foundations of the General Mathematical Theory*, Izd. Akad. Nauk SSSR, Moscow, 1963
⁹ Freudenthal A.M., Geiringer H. *The mathematical theories for inelastic continuum*, In: *Encyclopedia of Physics*, Ed. S. Flügge, VI, 1958
¹⁰ Love A.E.H. *A Treatise On The Mathematical Theory Of Elasticity*, Dover Publications, 1927
¹¹ Handelman, G. H.: *A variational principle for a state of combined plastic stress*. Quart. Appl. Math. 1 351-353, 1944
¹² Hill R., Siebel M. P. L.: *On the Plastic Distortion of Solid Bars by Combined Bending And Twisting*, Journal Of The Mechanics And Physics Of Solids, 1 207-214, 1953
¹³ Steele M. C.: *The Plastic Bending And Twisting of Square Section Members*, Journal of the Mechanics And Physics Of Solids, 8. 188-166, 1954
¹⁴ Gaydon F.A.: *On the Combined Torsion/Tension of a Partly Plastic Circular Cylinder*; Quart. Journal. Mech./Applied Math., V, 1, 29-41, 1952
¹⁵ Gaydon F.A., Nuttall H.: *On Combined Bending/Twisting of Beams of Various Sections*. Journal of the Mechanics/Physics of Solids, 6, 17-26, 1957
¹⁶ Sankaranarayanan, R., Hodge, P. G.: *On the Use of Linearized Yield Conditions for Combined Stresses in Beams*, Journal of the Mechanics and Physics of Solids, 7, 22-36, 1958
¹⁷ Imegwu E. O.: *Plastic Flexure and Torsion*, Journal Of The Mechanics And Physics Of Solids, 8, 111-146, 1960
¹⁸ Ishikawa H.: *Elasto-Plastic Stress Analysis of Prismatic Bar under Combined Bending and Torsion*, ZAMM 68, 17–30, 1973
¹⁹ Ali A. R. M.: *Plastic Deformation/Springback of Pre-loaded Rod under Subsequent Torsion*, IE (I) Journal. MC, 6, 26-30, 2005
²⁰ Życzkowski M.: *Combined Loadings in the Theory of Plasticity*, Springer, 1981
²¹ Eisenhart L.P. *An Introduction to Differential Geometry*. Princeton University Press, Princeton, 1940
²² Matejcek J., Brand P.C., Drews A.R., Krause A., Lowe-Ma C., *Residual stresses in cold-coiled helical compression springs for automotive suspensions measured by neutron diffraction. Materials Science and Engineering, A* 367, 306–311, 2004.

Fig. 8 — State of maximum plasticization during preset.

We use the index B to mark the geometry in the state at full stroke during preset. The line of action of the compression force F_B and of the torsion moment K_B is parallel to the axis of the helix. The curvature κ_B and the measure of tortuosity θ_B of stressed spring are given by the equations

$$(5.1) \quad \kappa_B = \frac{\cos^2 \alpha_B}{R_B}, \quad \theta_B = \frac{\sin \alpha_B \cos \alpha_B}{R_B},$$

where R_B, α_B are the radius and the angle of the helix in the state of full stroke B.

During the loading from the initial state A to final state B the deformation of the helical spring is accompanied by the plastic flow of material. Assuming, that the maximal curvature κ_B and the measure of tortuosity θ_B at the state of maximal plasticization B are given, the moments m_B and t_B at the state of maximal plasticization could be find from

$$(5.2) \quad M_p(\kappa_B - \kappa_A, \theta_B - \theta_A) = m_B, \quad T_p(\kappa_B - \kappa_A, \theta_B - \theta_A) = t_B,$$

The bending moment $M_p(\kappa_B - \kappa_A, \theta_B - \theta_A)$ and torque $T_p(\kappa_B - \kappa_A, \theta_B - \theta_A)$ are the functions of difference of curvature of the naturally curved bar during bending $\kappa_B - \kappa_A$ and difference of tortuosity $\theta_B - \theta_A$. The bending moment and torque relate to the local coordinate system of the cross-section of the wire.

The new configuration can be maintained by a wrench of which the axis is the axis of the helix, and the force F_B and couple K_B are given by the equations

$$(5.3) \quad t_B \cos \alpha_B - m_B \sin \alpha_B = R_B F_B,$$

$$t_B \sin \alpha_B + m_B \cos \alpha_B = K_B.$$

Fig. 9 – Elastic spring-back of helical spring and residual stresses after preset, and the residual stresses in helical springs after preset.

The moments during the elastic unloading from the state B to the intermediate state with the current curvature $0 < \kappa < \kappa_B$ and the measure of tortuosity $0 < \theta < \theta_B$ are

$$(5.1) \quad M_c(\kappa_B - \kappa, \theta_B - \theta) = m_B - EJ(\kappa_B - \kappa), T_c(\kappa_B - \kappa, \theta_B - \theta) = t_B - GJ_p(\theta_B - \theta).$$

We use the index C to mark the geometry in the unloaded state. For a bar which has been twisted and bended in constant ratio, the residual stresses after unloading are evaluated below. At the state of complete elastic unloading

$$\kappa_C = \frac{\cos^2 \alpha_C}{R_C}, \quad \theta_C = \frac{\sin \alpha_C \cos \alpha_C}{R_C} \text{ is the unloaded bending radius and } \theta_C \text{ is angle of twist/unit length of bar respectively.}$$

At the state of complete elastic unloading C helical spring is free and moments disappear. The conditions, that bending moment and torque vanish:

$$m_B - EJ(\kappa_B - \kappa_C) = 0, \quad t_B - GJ_p(\theta_B - \theta_C) = 0.$$

From these equations we obtain the resultant curvature and tortuosity of helical spring after preset:

$$\kappa_C = \kappa_B - \frac{m_B}{EJ}, \quad \theta_C = \theta_B - \frac{t_B}{GJ_p}.$$

RESIDUAL STRESSES IN HELICAL SPRINGS AFTER PRESET

In this section we study the preset by means of axial compression of the spring. The numerical calculation were performed for $R_A = R_B = 60 \text{ mm}$, $r = 7 \text{ mm}$, $\alpha_A = 0.3$, $\alpha_B = 0.1$. The resulted geometry of spring is characterized by the values $R_C = 60.47 \text{ mm}$, $\alpha_C = 0.145$.

The stresses components $\sigma_{zz}^B(\rho, \varphi)$, $\tau_{rz}^B(\rho, \varphi)$ in each point of the cross-section at the moment of maximal plasticization could be calculated using Eqs. (2.5) and (2.6).

The residual strains at the state of complete elastic unloading after preset could be obtained immediately subtracting the elastic stresses from stress components $\sigma_z^C(x, y)$, $\tau_{rz}^C(x, y)$ at the plastic state:

$$\sigma_{zz}^C(\rho, \varphi) = \sigma_{zz}^B(\rho, \varphi) - (\kappa_B - \kappa_C)E\rho \sin \varphi, \quad \tau_{rz}^C(\rho, \varphi) = \tau_{rz}^B(\rho, \varphi) - (\theta_B - \theta_C)G\rho.$$

With the expressions (48) for unloaded curvature and unloaded twist per unit length we get finally the expressions for residual stresses

$$\sigma_{zz}^C(\rho, \varphi) = \sigma_{zz}^B(\rho, \varphi) - \frac{\rho \sin \varphi}{J} m_B, \quad \tau_{rz}^C(\rho, \varphi) = \tau_{rz}^B(\rho, \varphi) - \frac{\rho}{J_p} t_B.$$

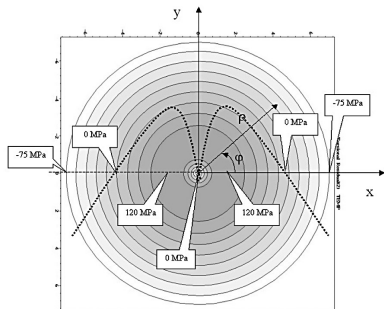


Figure 12: Residual shear $\tau_{rz}^C(\rho, \varphi)$ stress after preset

The residual stresses after preset exhibit Figures 12-14. The residual shear $\tau_{rz}^C(\rho, \varphi)$ (Fig.12) stress due to torsion depends mostly on radius ρ and demonstrates a weak dependence on polar angle φ . On the boundary of cross-section $\rho = r$ the shear stress is about -75 MPa and therefore reduces the in-service stresses. The bending stress $\sigma_{zz}^C(\rho, \varphi)$ is positive on the surface of boundary of cross-section $\rho = r$ at $\varphi = 0$. The stress $\sigma_{zz}^C(\rho, \varphi)$ is negative on the surface of boundary of cross-section $\rho = r$ at $\varphi = \pi$ (Fig.13).

The pattern of equivalent residual stress $\sqrt{(\sigma_{zz}^C(\rho, \varphi))^2 + 3(\tau_{rz}^C(\rho, \varphi))^2}$ is similar to shear stress (Fig.14).

The equivalent residual stress depends mostly on radius ρ and demonstrates a weak dependence on polar angle φ . The total shear stress is the sum of the in-service shear stress $4M/\pi r^3$ and residual stress $\tau_{rz}^C(\rho, \varphi)$, such that

$$\tau(r) = \frac{4M}{\pi r^3} + \tau_{rz}^C(\rho, \varphi).$$

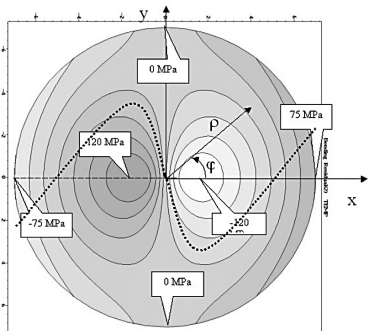


Figure 13: Residual normal stress $\sigma_{zz}^C(\rho, \varphi)$ after preset

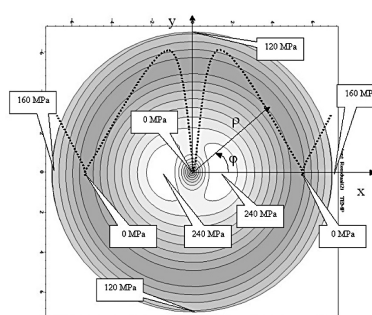


Figure 14: Residual equivalent stress after preset

On the outer surface of the wire the technologically admissible residual stress is approximately constant. Residual shear stresses site in sign to the in-service load stress, thus clearly improving fatigue properties.